The RNA-binding protein Sam68 modulates the alternative splicing of Bcl-x

Maria Paola Paronetto,[1,2] Tilman Achsel,[2] Autumn Massiello,[3,4] Charles E. Chalfant,[3,4] and Claudio Sette[1,2]

[1]Department of Public Health and Cell Biology, Section of Anatomy, University of Rome Tor Vergata, 00133 Rome, Italy
[2]Laboratory of Neuroembryology, Institute of Experimental Neuroscience, Fondazione Santa Lucia Istituto di Ricovero e Cura a Carattere Scientifico, 00143 Rome, Italy
[3]Department of Biochemistry, Virginia Commonwealth University, Richmond, VA 23298
[4]Research and Development, Hunter Holmes McGuire Veterans Administration Medical Center, Richmond, VA 23249

The RNA-binding protein Sam68 is involved in apoptosis, but its cellular mRNA targets and its mechanism of action remain unknown. We demonstrate that Sam68 binds the mRNA for Bcl-x and affects its alternative splicing. Depletion of Sam68 by RNA interference caused accumulation of antiapoptotic Bcl-x(L), whereas its up-regulation increased the levels of proapoptotic Bcl-x(s). Tyrosine phosphorylation of Sam68 by Fyn inverted this effect and favored the Bcl-x(L) splice site selection. A point mutation in the RNA-binding domain of Sam68 influenced its splicing activity and subnuclear localization. Moreover, co-expression of ASF/SF2 with Sam68, or fusion with an RS domain, counteracted Sam68 splicing activity toward Bcl-x. Finally, Sam68 interacted with heterogenous nuclear RNP (hnRNP) A1, and depletion of hnRNP A1 or mutations that impair this interaction attenuated Bcl-x(s) splicing. Our results indicate that Sam68 plays a role in the regulation of Bcl-x alternative splicing and that tyrosine phosphorylation of Sam68 by Src-like kinases can switch its role from proapoptotic to antiapoptotic in live cells.

Introduction

Alternative splicing is a regulatory mechanism that allows genes to encode for multiple protein isoforms that often play different biological roles (Maniatis and Tasic, 2002; Black, 2003; Stetefeld and Ruegg, 2005). It arises from the optional use of alternative splice sites within a pre-mRNA. In mammals, the signals that define the beginning and the end of an intron are ill defined, and the authentic splice sites can be identified only with the help of additional cis-acting elements, named "splicing enhancers" and "splicing silencers." Usually, any given region of a pre-mRNA contains, in addition to various potential exon–intron boundaries, several splicing enhancers and silencers that antagonize each other (Black, 2003). This enormous body of information is decoded by two families of RNA-binding proteins: the serine/arginine (SR) proteins and the heterogenous nuclear RNPs (hnRNPs; Black, 2003; Matlin et al., 2005). The SR proteins consist of one or two RNA-binding domains and a domain rich in SR dipeptides. They bind to splicing enhancers and usually activate splicing at nearby splice sites. The hnRNPs bind mostly, but not always, to splicing silencers and therefore inhibit splicing at nearby splice sites. Thus, the fate of a pre-mRNA region is usually decided by the antagonism between hnRNP and SR proteins (for review see Matlin et al., 2005). The best-described example is the antagonism between the SR protein ASF/SF2 and hnRNP A1. The ratio of ASF/SF2 to hnRNP A1 determines the usage of splice sites, because ASF/SF2 recruits the U1 small nuclear RNP to the pre-mRNA, a crucial step in establishing a 5′ splice site, whereas hnRNP A1 counteracts U1 binding (Eperon et al., 2000). However, the limited number of hnRNP and SR proteins, as well as their limited binding specificity for the pre-mRNAs, cannot faithfully determine splicing in so many pre-mRNAs (Singh and Valcarcel, 2005). Additional proteins are likely required to confer specificity to the regulation of alternative splicing in live cells and to decipher the signaling pathways triggered by environmental cues.

A well-suited candidate to integrate signal transduction pathways and RNA metabolism is Sam68. This RNA-binding protein belongs to the signal transduction and activation of RNA (STAR) metabolism family (Vernet and Artzt, 1997; Lukong and Richard, 2003), and it was first identified as a target of the tyrosine kinase Src (Fumagalli et al., 1994; Taylor and Shalloway, 1994). STAR proteins are characterized by a KH

Correspondence to Claudio Sette: claudio.sette@uniroma2.it

Abbreviations used in this paper: GSG, GRP33/Sam68/GLD1; hnRNP, heterogenous nuclear RNP; SR, serine/arginine; STAR, signal transduction and activation of RNA.

The online version of this article contains supplemental material.

The Journal of Cell Biology, Vol. 176, No. 7, March 26, 2007 929–939
http://www.jcb.org/cgi/doi/10.1083/jcb.200701005

Supplemental Material can be found at:
http://www.jcb.org/cgi/content/full/jcb.200701005/DC1

(hnRNP K homology) domain embedded in a highly conserved region called GSG (GRP33/Sam68/GLD1) domain, which is required for homodimerization and sequence-specific RNA binding (Lin et al., 1997; Chen et al., 1999). Sam68 has been implicated in the regulation of cell cycle progression and apoptosis (Taylor et al., 2004; Babic et al., 2006). The subcellular localization and the affinity of Sam68 for RNA are regulated by posttranslational modifications, like phosphorylation and methylation (Wang et al., 1995, Cote et al., 2003; Paronetto et al., 2003; Lukong et al., 2005). The localization of Sam68 is predominantly nuclear, suggesting a function in pre-mRNA processing. A role for Sam68 in alternative splicing was demonstrated by its ability to induce inclusion of the variable exon v5 in the CD44 mRNA (Matter et al., 2002). The activation of Ras in response to phorbol ester stimulation triggered the phosphorylation of Sam68 by Erk1/2 and Sam68-dependent v5 inclusion in mouse T-lymphoma cells. More recently, it has been observed that Sam68 cooperates with the splicing activator SRm160 in the regulation of CD44 alternative splicing (Cheng and Sharp, 2006). In addition, Sam68 was found to associate with Brm, a component of the SWI/SNF chromatin remodeling complex (Batsché et al., 2006), suggesting that it may participate in splicing events during the initial stages of CD44 pre-mRNA synthesis. Aside from CD44 alternative splicing, no information is available on other pre-mRNAs that could be regulated by this protein. Given the role of Sam68 in the regulation of apoptosis, it would be important to identify cellular targets involved in such a process.

Alternative splicing plays a crucial role in the control of apoptosis. Several pre-mRNAs for cell death factors are alternatively spliced, yielding isoforms with opposing functions during programmed cell death (Schwerk and Schultze-Osthoff, 2005). A clear example is the Bcl-x transcript, which is alternatively spliced to produce the antiapoptotic Bcl-x(L) or the proapoptotic Bcl-x(s) (Boise et al., 1993). The choice of alternative splicing of Bcl-x pre-mRNA reflects the sensitivity of cells toward agents that induce apoptosis. For example, cancer cells often up-regulate the antiapoptotic Bcl-x(L) isoform, and this event is associated with increased risk of metastasis, reduced sensitivity to chemotherapeutic treatments, and poor prognosis (Clarke et al., 1995; Olopade et al., 1997). On the other hand, treatment of cancer cells expressing high levels of Bcl-x(L) with antisense oligonucleotides complementary to the Bcl-x(L) splice site favor the expression of Bcl-x(s) and sensitize cells to undergo apoptosis (Mercatante et al., 2002). These observations strongly indicate that manipulation of Bcl-x alternative splicing may have important applications in cancer treatment. However, despite the crucial importance of this process, little information is available on splicing regulators controlling splice site selection of Bcl-x pre-mRNA. Recent reports have shown that hnRNP F/H induce Bcl-x(s) expression (Garneau et al., 2005), whereas SAP155 is required for selection of the Bcl-x(L) splice site (Massiello et al., 2006). Moreover, the ratio between the two isoforms can be shifted toward Bcl-x(s) by an increase in ceramide (Chalfant et al., 2002). Hence, cells can quickly switch to an apoptotic program as a consequence of altered growth conditions through a change in splice site selection of the Bcl-x pre-mRNA.

In the present work, we have investigated the role of the RNA-binding protein Sam68 in the regulation of apoptosis. We have identified the first cellular targets of Sam68 involved in apoptosis and provide evidence that Sam68 favors the selection of the Bcl-x upstream 5′ splice site and the production of the proapoptotic Bcl-x(s) isoform.

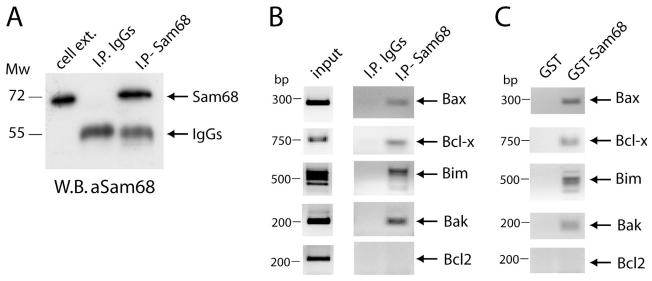

Figure 1. **Endogenous Sam68 associates with the mRNAs encoding for regulators of apoptosis.** 1 mg of HEK293 cell extracts was immunoprecipitated with 10 μg of either control rabbit IgGs or anti-Sam68 IgGs as described in Materials and methods. An aliquot of the immunoprecipitated proteins was analyzed in Western blot for the presence of Sam68 (A), and the remaining sample was extracted in phenol/chloroform after treatment with proteinase K and DNase. (B) Extracted RNA was retrotranscribed and used for PCR amplification with oligonucleotides specific for the indicated genes. (C) GST pull-down experiment using purified GST or GST-Sam68 immobilized on glutathione-agarose beads and 100 μg of total RNA extracted and purified from HEK293 cells. Adsorbed RNA was extracted, retrotranscribed, and amplified as described in B.

Results

Sam68 directly binds mRNAs for regulators of apoptosis

Sam68 is a RNA-binding protein whose intracellular levels regulate cell cycle progression and apoptosis (Taylor, et al., 2004; Babic, et al., 2006). We set out to investigate whether Sam68 plays a direct role on the posttranscriptional regulation of mRNAs encoding known apoptotic regulators. Endogenous Sam68 was immunoprecipitated with an anti-Sam68 antibody from HEK293 cell extracts (Fig. 1 A) prepared under conditions that preserve RNA and RNPs (Paronetto et al., 2006). RNA was extracted from the immunoprecipitates and analyzed by RT-PCR for the presence of genes involved in the regulation of apoptosis. We found that Sam68 specifically binds to the endogenous Bak, Bax, Bcl-x, and Bim mRNAs, but not to Bcl2 mRNA. Control immunoprecipitations with preimmune IgGs gave no enrichment in any of the mRNAs analyzed (Fig. 1 B). To test whether Sam68 can recognize these mRNAs on its own, we purified GST-Sam68 from bacteria and total RNA from HEK293 cells and performed GST pull-down experiments. RT-PCR analysis showed that Sam68 can directly bind to these mRNAs in a cell-free assay (Fig. 1 C).

Sam68 enhances Bcl-x(s) splicing in vivo

To date, the only cellular target identified for the splicing activity of Sam68 is CD44 (Matter et al., 2002). Because Sam68 binds to the mRNA for Bcl-x, an apoptotic regulator known to undergo alternative splicing (Boise et al., 1993), posttranscriptional

regulation of this mRNA by Sam68 was investigated further. Alternative splicing is usually governed by a delicate balance of activators and inhibitors of splice site selection that have redundant functions in the cell (Matlin et al., 2005; Singh and Valcarcel, 2005). Hence, we investigated whether changes in the intracellular concentration of Sam68 modulate the alternative splicing of Bcl-x in HEK293 cells. We found that down-regulation of Sam68 by RNAi changed the ratio of alternatively spliced Bcl-x isoforms, with an increase in the antiapoptotic Bcl-x(L) and a decrease in the proapoptotic Bcl-x(s) transcript (approximately twofold; Fig. 2 A, right). A decrease in Bcl-x(s) was observed also at the protein level after depletion of Sam68 (Fig. 2 A, left).

As a second approach, we overexpressed GFP or GFP-Sam68 constructs in HEK293 cells. GFP-positive cells were sorted, and cellular extracts were prepared for RT-PCR and Western blot analyses. Up-regulation of Sam68 caused an increase in the Bcl-x(s)/Bcl-x(L) ratio at the mRNA level (4.5-fold; Fig. 2 B). A similar increase in ratio was obtained by transfection of HEK293 cells with a Bcl-x(L) antisense oligonucleotide (3.8-fold; Fig. 2 B). Up-regulation of Sam68 also increased Bcl-x(s) protein (Fig. 2 B). These results demonstrate that fluctuations in the intracellular concentration of Sam68 affect the alternative splicing of endogenous Bcl-x mRNA.

Sam68 enhances splicing of the Bcl-x minigene in a dose-dependent manner

To investigate the regulation of Bcl-x splicing by Sam68 in more detail, we used a Bcl-x minigene that spans the whole alternatively spliced region from exon 1 to 3, with a shortened intron 2 (Fig. 2 C; Massiello, et al., 2004). Cotransfection of GFP-Sam68 with this reporter strongly enhanced the formation of the short variant of the Bcl-x transcript with respect to transfection of GFP alone (Fig. 2 C). The selection of the upstream 5′ splice site in exon 2 was stimulated in a dose-dependent manner when the Bcl-x minigene was cotransfected with increasing amounts of GFP-Sam68 (Fig. 2 D). Hence, the Bcl-x minigene recapitulates the effects of Sam68 on the endogenous Bcl-x mRNA.

MAPK signaling does not affect Sam68-mediated Bcl-x alternative splicing

Phosphorylation of Sam68 by the MAPK Erk1/2 induces inclusion of exon v5 in the CD44 mRNA (Matter et al., 2002). To determine the effects of Erk1/2 signaling on Sam68-mediated splicing of Bcl-x, HEK293 cells were transfected with GFP or GFP-Sam68 and treated with selective inhibitors of the MAPK pathway. We observed that neither U0126, which blocks activation of Erk1/2 by MEK, nor JNK inhibitor 1, which blocks activation of the JNK family of MAPKs that are also involved in alternative splicing (Pelisch et al., 2005), substantially affected Sam68-mediated selection of the 5′ splice site in the Bcl-x minigene (Fig. S1 B, available at http://www.jcb.org/cgi/content/full/jcb.200701005/DC1). Under these conditions, the localization of GFP-Sam68 was also not affected (Fig. S1 A).

To determine whether constitutive activation of Erk1/2 signaling affected Sam68-mediated Bcl-x alternative splicing,

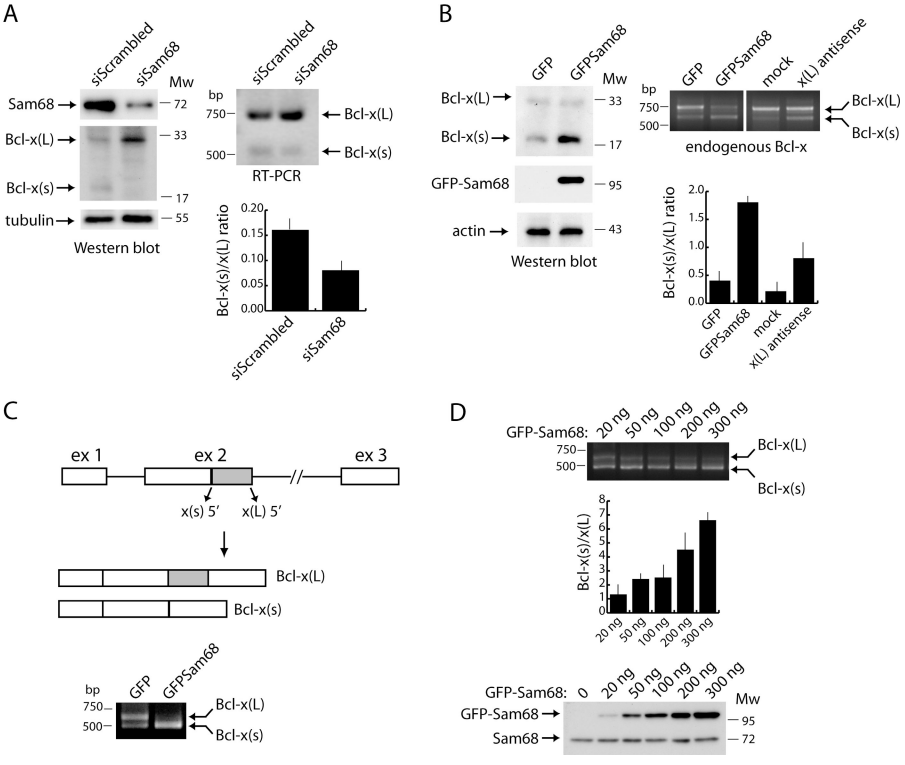

Figure 2. **Fluctuations in the intracellular levels of Sam68 affect the alternative splicing of Bcl-x.** (A) Knock down of Sam68 in HEK293 cells was obtained by RNAi and verified by Western blot analysis (top left). Samples were also stained with anti-Bcl-x (middle) and anti-tubulin (bottom). Total RNA was extracted from these samples, and expression of Bcl-x alternatively spliced forms was determined by RT-PCR (top right). Densitometric analysis of the Bcl-x(s)/Bcl-x(L) ratio in three independent experiments was performed, and results are shown below the panel. (B) HEK293 cells were transfected with GFP or GFP-Sam68 and GFP-positive cells (left) or with a Bcl-x(L) antisense oligo (right). GFP-expressing cells were isolated by cell sorting. Analysis of Bcl-x mRNAs by RT-PCR is shown in the right panel. Densitometric analysis of the Bcl-x(s)/Bcl-x(L) ratio in three separate experiments was performed, and results are shown below the panel. Western blot analysis of GFP-Sam68 and of the Bcl-x isoforms are shown in the left panels. Actin staining of the blot was used as internal loading control. (C) Schematic diagram of the Bcl-x minigene used. HEK293 were transfected with 0.5 μg pCDNA3.1-Bcl-x minigene and 0.5 μg GFP-Sam68 or GFP as control. The effect on alternative splicing was detected by RT-PCR (panel below the scheme). (D) 0.5 μg pCDNA3.1-Bcl-x minigene and different amounts of GFP-Sam68 (0.02–0.3 μg) were also transfected. Cells were harvested 20 h later. RT-PCR of the samples was performed to determine the relative abundance of Bcl-x(L) and Bcl-x(s) mRNAs by densitometric analysis. Mean values ± SD of three independent experiments are shown. Anti-Sam68 Western blot (bottom) indicates the expression levels of endogenous (Sam68) and recombinant (GFP-Sam68) proteins.

HEK293 cells were cotransfected with MEKK1 and suboptimal concentration of GFP-Sam68 (Fig. S1 D). Under these conditions, Erk1/2 was activated by MEKK1 (Fig. S1 C, left). Interestingly, activation of Erk1/2 signaling caused a partial redistribution of GFP-Sam68 in the cytoplasm (Fig. S1 A). Analysis of immunoprecipitated GFP or GFP-Sam68 by Western blot with phosphospecific antibodies indicated that MEKK1 increased phosphorylation of Sam68 at serines, whereas threonine phosphorylation was already detected under basal conditions and only mildly affected by MEKK1 (Fig. S1 C, right). Sam68-mediated induction of Bcl-x(s) alternative splicing was only marginally affected in the presence of activated Erk1/2 (2.59 vs. 2.04 in the x(s)/x(L) ratio; Fig. S1 D, left). To rule out the possibility that the basal threonine phosphorylation of Sam68 was sufficient to modulate its activity, a similar experiment was performed using wild-type myc-Sam68 or -Sam68m1, a mutated version lacking the eight Erk1/2 phosphorylation sites of Sam68 (Matter et al., 2002). As illustrated in Fig. S1 D, we observed that myc-Sam68m1 was as efficient as the wild-type protein to favor the Bcl-x(s) 5′ splice site selection. These results indicate that, different from what was observed with CD44, Erk1/2 signaling does not affect Sam68-mediated Bcl-x alternative splicing.

The tyrosine kinase Fyn modulates Sam68-mediated alternative splicing of Bcl-x mRNA

Sam68 was originally identified as a substrate of Src in mitosis (Fumagalli et al., 1994; Taylor and Shalloway, 1994), and tyrosine phosphorylation of Sam68 by the Src-like kinase Fyn decreases its affinity for synthetic homopolymeric RNA in vitro (Wang et al., 1995). Hence, we asked whether tyrosine phosphorylation affected the splicing activity of Sam68 toward a cellular target. Coexpression of wild-type Fyn counteracted the ability of GFP-Sam68 to favor the Bcl-x(s) 5′ splice site selection, resulting in an isoform ratio similar to the GFP control (Fig. 3 B). Remarkably, the constitutively active mutant Fyn_{Y528F} (Sette et al., 2002), which induces a stronger tyrosine phosphorylation of Sam68 (Fig. 3 B), completely reverted the effect and induced predominant selection of the Bcl-x(L) 5′ splice site in a Sam68-dependent manner (Fig. 3 B, bar graph). Both Fyn and Fyn_{Y528F} caused the relocalization of Sam68 from a diffuse distribution in the nucleoplasm to discrete subnuclear foci (Fig. 3 A). No effect of Fyn on Bcl-x splicing were observed when Sam68 was not overexpressed. Because the endogenous Sam68 was not strongly tyrosine phosphorylated under these conditions (20 h after transfection), we performed splicing assays after prolonged Fyn expression. Remarkably, tyrosine phosphorylation of the endogenous Sam68 was strongly increased 48 h after transfection of Fyn (Fig. 3 C). In these cells, the effects of Fyn on Bcl-x minigene splicing were similar to those obtained with overexpressed Sam68 (Fig. 3 C), indicating that tyrosine phosphorylation of endogenous Sam68 affects Bcl-x splicing. Moreover, a similar regulation of Bcl-x isoform ratio was also observed with endogenous mRNAs (Fig. S2, available at http://www.jcb.org/cgi/content/full/jcb.200701005/DC1). Next, we asked whether

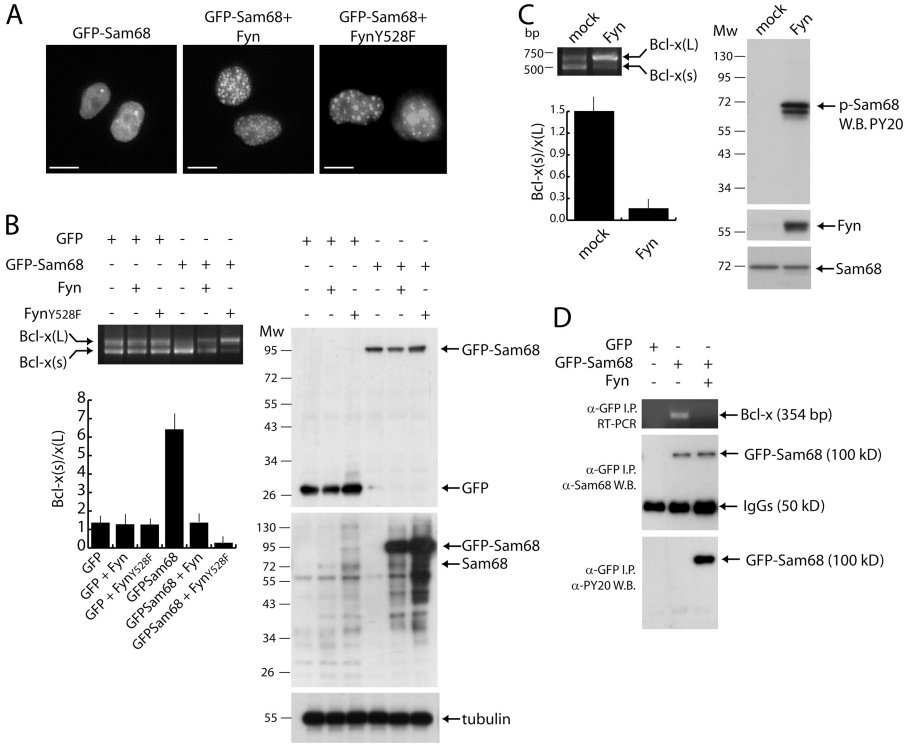

Figure 3. **Tyrosine phosphorylation of Sam68 by Fyn modulates the alternative splicing of Bcl-x.** (A) Live-cell images of HEK293 cells transfected with wild-type GFP-Sam68 either alone or in combination with Fyn or FynY528F, as indicated. Bars, 10 μm. (B) Splicing assay of the Bcl-x minigene (0.5 mg) in HEK293 cells transfected with 0.25 mg of either GFP or GFP-Sam68 alone or in combination with 0.25 mg Fyn or FynY528F. Cells were harvested 20 h after transfection and processed for RT-PCR. Densitometric analysis of three independent experiments are shown below the image (mean values ± SD of the Bcl-x(s)/Bcl-x(L) ratio). Cell extracts of the same samples were analyzed in Western blot for GFP (top), tyrosine phosphorylation with the PY20 antibody (middle; position of recombinant GFP-Sam68 and of endogenous Sam68 are indicated by arrows), and tubulin as loading control (bottom). (C) HEK293 cells were transfected with the Bcl-x minigene and empty pCMV5 (mock) or pCMV5-Fyn (Fyn). After 48 h, cells were harvested and used for Bcl-x RT-PCR (left) or Western blot analysis as in B. Bcl-x(s)/x(L) ratio of three independent experiments is shown in the bar graph. (D) Coimmunoprecipitation of Sam68 with Bcl-x endogenous mRNA from HEK293 cells transfected with GFP or GFP-Sam68 either alone or in combination with Fyn to induce tyrosine phosphorylation. Cell extracts were immunoprecipitated with the GFP antibody, and coprecipitated RNA was extracted and used for RT-PCR (top). An aliquot of the immunoprecipitates was saved for Western blot analysis of Sam68 (middle) and of tyrosine phosphorylation (bottom).

tyrosine phosphorylation by Fyn also affected the binding of Sam68 to the endogenous Bcl-x mRNA. Bcl-x mRNA was coimmunoprecipitated with GFP-Sam68 but not with GFP (Fig. 3 D). Coexpression of Fyn abolished binding of Bcl-x mRNA to GFP-Sam68 (Fig. 3 D), indicating that tyrosine phosphorylation reduces the affinity of Sam68 for this cellular target in live cells.

A novel mutation in the RNA-binding domain of Sam68 affects Bcl-x splicing

A specific mutation (V276F) in the GSG domain of the Sam68 homologue GLD-1 (Jones and Schedl, 1995) affects germ cell apoptosis after DNA damage in *Caenorhabditis elegans* (Schumacher et al., 2005). Because this valine residue (V229) is conserved in human Sam68, we generated the homologous mutant allele (GFP-Sam68$_{V229F}$) and tested its activity toward Bcl-x splicing. First, the RNA-binding activity was tested in vitro by pull-down assays with synthetic homopolymeric RNA. Both wild-type and mutant Sam68 bound to polyU-Sepharose beads with approximately the same affinity (see Fig. 6 B). By contrast, Sam68$_{V229F}$ was defective in binding to polyA–Sepharose beads (see Fig. 6 B), indicating that this mutation affects the RNA-binding specificity of the protein. To test the effect on splicing, wild-type and mutant GFP-Sam68 were coexpressed with the Bcl-x minigene. Remarkably, Sam68$_{V229F}$ was completely unable to favor the selection of the Bcl-x(s) 5′ splice site. Rather, its expression enhanced the selection of the Bcl-x(L) 5′ splice site (Fig. 4 B). Moreover, unlike the wild-type protein, Sam68$_{V229F}$ was unable to favor the expression of the endogenous Bcl-x(s) mRNA (Fig. 4 C). Densitometric analysis (Fig. 4 D) and real-time PCR quantification (Fig. 4 E) of RNA coimmunoprecipitation experiments showed that Sam68$_{V229F}$ was partially defective in binding to endogenous Bcl-x mRNA. Interestingly, we also observed that Sam68$_{V229F}$ localized to discrete nuclear foci and was not diffused in the nucleoplasm like wild-type Sam68 (Fig. 4 A). Confocal microscopy showed that these foci were different from the speckles where splicing factors like SC35 and ASF/SF2 accumulate (Fig. S3, available at http://www.jcb.org/cgi/content/full/jcb.200701005/DC1). On the other hand, the localization of Sam68$_{V229F}$ was similar to that observed when wild-type Sam68 was coexpressed with activated Fyn. Because in both conditions the Bcl-x(L) 5′ splice site was favored, these results suggest an inverse correlation between splice site modulation by Sam68 and its localization to subnuclear foci. Importantly, Sam68$_{NLS\text{-}KO}$, in which two arginine residues in the nuclear localization signal (Wu et al., 1999) were substituted (R436A/R442A), did not affect splicing of Bcl-x (compared with GFP alone), indicating that nuclear localization of Sam68 is required to modulate splice site selection of Bcl-x pre-mRNA (Fig. 4, A and B).

Modulation of Bcl-x splicing by Sam68 correlates with its ability to induce apoptosis

Next, the correlation between Sam68 activity toward Bcl-x splicing and induction of apoptosis was investigated. Similar to what is reported in NIH3T3 cells (Taylor et al., 2004), up-regulation of Sam68 induced apoptosis in HEK293 cells, as determined by annexin V binding (Fig. 5 A), nuclear fragmentation (Fig. 5 B), and cleavage of caspase 3 (Fig. 5 C). Induction of apoptosis was similar to that elicited by transfection of the Bcl-x(L) antisense oligonucleotide (Fig. 5 A), which affects the Bcl-x(s)/Bcl-x(L) ratio similarly to Sam68 (Fig. 2 B). On the other hand, Sam68$_{V229F}$ and Sam68$_{NLS\text{-}KO}$, which did not induce Bcl-x(s), were unable to trigger apoptosis in the same experimental setting. These results indicate that modulation of Bcl-x alternative splicing by Sam68 strongly correlates with the ability of the protein to elicit an apoptotic response.

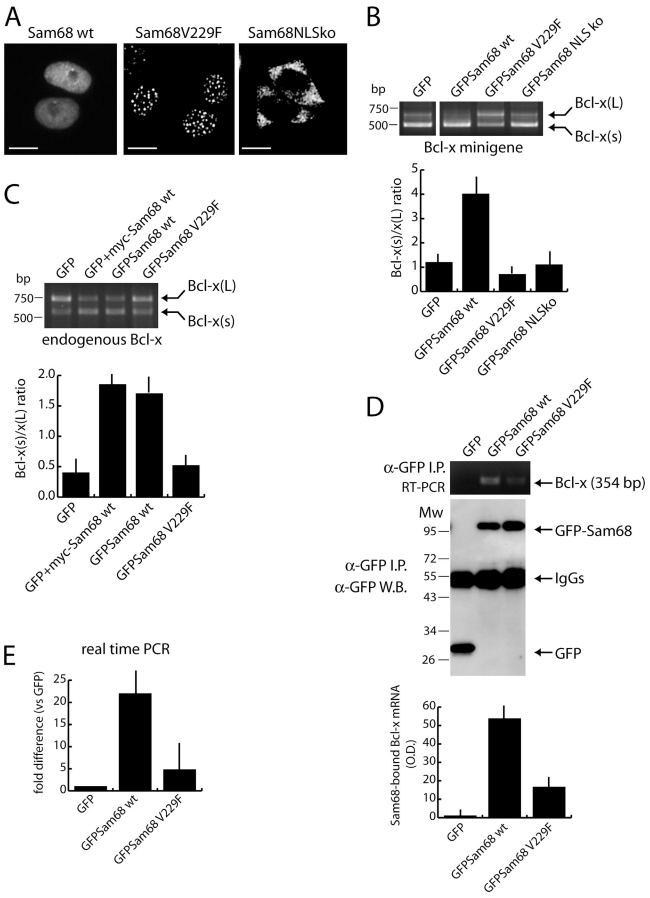

Figure 4. **The V229F mutation in the GSG domain of Sam68 affects Bcl-x alternative splicing.** (A) Live-cell images of HEK293 cells transfected with mutant GFP-Sam68 constructs as indicated. Bars, 10 μm. (B) Splicing assay of the Bcl-x minigene in HEK293 cells transfected with the indicated constructs. Cells were harvested 20 h after transfection and processed for RT-PCR. The bar graph represents mean values ± SD of the Bcl-x(s)/Bcl-x(L) ratio from three independent experiments. (C) RT-PCR analysis of endogenous Bcl-x mRNA isoforms in HEK293 cells transfected with wild-type or mutant GFP-Sam68 and sorted for GFP. The panel is a representative experiment. The bar graph represents mean values ± SD of the Bcl-x(s)/Bcl-x(L) ratio from three independent experiments. (D) Extracts from HEK293 cells transfected with the indicated constructs were immunoprecipitated with anti-GFP antibody, and coprecipitated RNA was extracted and used for conventional RT-PCR (top). An aliquot of the immunoprecipitates was analyzed by Western blot (bottom). Densitometric analysis of the RT-PCR from three independent experiments is shown in the bar graph (mean values ± SD). (E) Samples described in D were analyzed by quantitative real-time PCR. The bar graph represents the mean ± SD of three experiments. Data are presented as ratio of the value: GFP-Sam68/GFP.

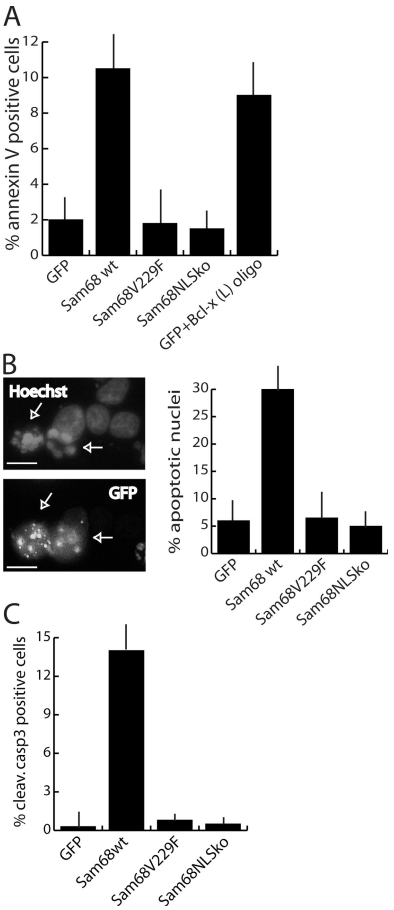

Figure 5. **Sam68-mediated alternative splicing of Bcl-x correlates with induction of apoptosis.** (A) HEK293 cells were transfected with the indicated constructs and harvested after 48 h to be processed for annexin V–PE staining. The percentage of annexin V–positive cells is referred to the GFP-positive population. Data are the mean ± SD of three separate experiments. (B and C) HEK293 cells transfected as in A were examined 72 h after transfection. Nuclear fragmentation (B), judged as indicated by the two cells indicated by arrows in the left panels, was scored in the GFP-positive cells. Data were obtained by counting at least 200 cells for each sample in five different fields and represent the mean ± SD of three separate experiments. Bars, 10 μm. (C) The bar graph represents the percentage of cells positive in immunofluorescence for the activated (cleaved) caspase 3 in the GFP-positive population. The results are the mean ± SD of three independent experiments (at least 500 cells for each sample were counted in each experiment).

Opposite actions of Sam68 and the SR protein ASF/SF2 in Bcl-x alternative splicing

Our results demonstrate that Sam68 affects the choice of Bcl-x splice sites in live cells. Normally, the Bcl-x(L) isoform is expressed predominantly. Sam68 could either antagonize or favor the recruitment of SR proteins in the vicinity of the Bcl-x splice sites. To test these hypotheses, we attempted to shift the balance between Sam68 and SR proteins. Our previous results already showed that silencing Sam68 by RNAi increased Bcl-x(L) splicing (Fig. 2 A). Next, we checked whether up-regulation of ASF/SF2, a prototypical SR protein that is essential for cell survival (Li et al., 2005), exerted the same effect. Indeed, coexpression of ASF/SF2 induces virtually exclusive usage of the Bcl-x(L) splice site in the reporter minigene. When GFP-Sam68 is also expressed, ASF/SF2 prevails but the Bcl-x(L) is no longer exclusively selected. Up-regulation of ASF/SF2 did not affect the diffuse localization of GFP-Sam68 in HEK293 cells (Fig. 6 A). This result suggests that Sam68 does not function by recruiting SR proteins to the Bcl-x(s) splice site. If this is true, forced recruitment of a RS domain by Sam68 should not improve its splicing activity. To confirm this, we artificially fused the RS domain of ASF/SF2 to GFP-Sam68. The resulting fusion protein retains its RNA-binding activity, as measured by polyA and polyU pull-down assays (Fig. 6 B), indicating that its RNA-binding motif is not aberrantly folded. Nevertheless, the in vivo splicing assay indicated that the RS domain neutralized, rather than increased, the splice site modulating activity of Sam68 (Fig. 6 C). Interestingly, GFP-Sam68-RS was only partially diffused in the nucleoplasm, whereas a portion of the protein accumulated in foci similar to those observed with GFP-$Sam68_{V229F}$ (Fig. 6 A) but different from SC35 and ASF/SF2 speckles (Fig. S3).

Next, we investigated the effect of the coexpression of Sam68 and ASF/SF2 on apoptosis. Remarkably, we found again a close correlation between Bcl-x splicing and apoptosis. ASF/SF2 up-regulation almost completely suppressed the number of annexin V–positive cells (Fig. 6 D) and nuclear fragmentation (Fig. 6 E). In line with their effect on Bcl-x splicing, expression of GFP-Sam68-RS or coexpression of ASF/SF2 with Sam68 strongly reduced the number of apoptotic cells.

Sam68 interacts with hnRNP A1 in HEK293 cells

Alternative splicing is regulated by the concerted action of several splicing regulators (Matlin et al., 2005). To investigate whether Sam68 interacted with other splicing factors in HEK293 cells, the endogenous protein was immunoprecipitated, and the presence of associated factors was tested by Western blot analysis. As shown in Fig. 7 B, endogenous Sam68 did not interact with SAP155 and hnRNP F/H, two splicing regulators that were recently reported to affect Bcl-x alternative splicing (Garneau et al., 2005; Massiello et al., 2006), or with ASF/SF2. By contrast, we found that Sam68 specifically interacted with hnRNP A1, a splicing regulator known to antagonize the function of ASF/SF2 (Eperon et al., 2000). A similar interaction with hnRNP A1 was also observed with transfected Sam68 (Fig. 7 C). Confocal microscopy showed that GFP-Sam68 and hnRNP A1 were both diffused in the nucleoplasm and that they partially colocalized in some nuclear foci (Fig. 7 A, arrows). On the other hand, neither colocalization (Fig. 7 A) nor interaction (Fig. 7, B and C) was observed between ASF/SF2 and Sam68. The association between Sam68 and hnRNP A1 was only slightly affected by RNase treatment (Fig. 7 D). To confirm a protein–protein interaction between them, we performed pull-down assays. Bacterially purified GST fusion proteins containing different regions of Sam68 were incubated in vitro with HEK293 nuclear extracts. As shown in Fig. 7 E, hnRNP A1 strongly bound to the C-terminal region of Sam68 (276–443), which does not contain the RNA-binding domain. The minimal region required for binding was mapped to the last 93 amino acids of Sam68 (351–443). On the other hand, the N-terminal region of Sam68 (1–277), containing the whole GSG domain,

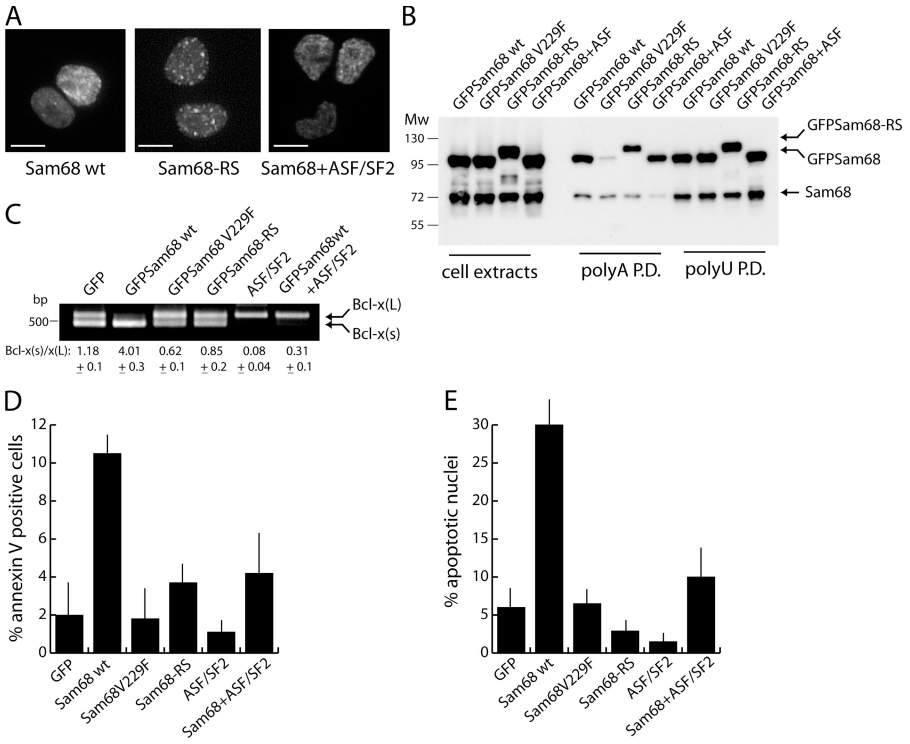

Figure 6. **Opposite actions of Sam68 and ASF/SF2 in Bcl-x alternative splicing.** (A) Live-cell images of HEK293 cells transfected with the indicated constructs encoding GFP-Sam68 variants and ASF/SF2. Bars, 10 μm. (B) Extracts from HEK293 cells transfected as indicated were incubated with either polyA- or polyU-Sepharose beads, and adsorbed proteins were analyzed in Western blot with the anti-Sam68 antibody. (C) Splicing assay of the Bcl-x minigene in HEK293 cells transfected with the indicated constructs. Cells were harvested 20 h after transfection and processed for RT-PCR. The experiment shown is representative of three independent experiments. Mean values ± SD of the Bcl-x(s)/Bcl-x(L) ratio are shown below the panel. (D) HEK293 cells were transfected with the indicated constructs and harvested after 48 h (for annexin V–PE staining) or (E) counted 72 h (for nuclear fragmentation) after transfection. Annexin V staining and nuclear fragmentation were assessed as described in the legend to Fig. 6. Data are the mean ± SD of three separate experiments.

weakly bound to hnRNP A1, suggesting that weak interaction through a common RNA could also occur. No binding to GST alone was observed. These results indicate that Sam68 and hnRNP A1 can form a protein–protein interaction.

To test whether association between Sam68 and hnRNP A1 was inhibited by conditions in which Bcl-x(L) splicing was favored, we tested the coimmunoprecipitation in the presence of Fyn or with GFP-Sam68 mutant proteins. Remarkably, we found that neither GFP-Sam68$_{V229F}$ nor GFP-Sam68-RS was able to associate (Fig. 8 A) or colocalize (Fig. S3) with hnRNP A1 and that this interaction was strongly reduced when wild-type Sam68 was phosphorylated on tyrosine by coexpression of Fyn (Fig. 8 A). To determine whether hnRNP A1 expression influences the Sam68 effects, we depleted hnRNP A1 by RNAi. HEK293 was transfected with hnRNP A1 siRNAs or scrambled controls 24 h before transfection with the Bcl-x minigene and GFP or GFP-Sam68. We observed that depletion of hnRNP A1 attenuated Sam68-induced Bcl-x(s) splicing (Fig. 8 B). Remarkably, annexin V staining indicated that depletion of hnRNP A1 also reduced the number of apoptotic cells elicited by Sam68 transfection (Fig. 8 C). These results suggest that hnRNP A1 and Sam68 cooperate to modulate the alternative splicing of Bcl-x and apoptosis in live cells (Fig. 8 D).

Discussion

The RNA-binding protein Sam68 has recently been proposed to regulate apoptosis (Taylor et al., 2004; Babic et al., 2006). However, no direct evidence on the mRNAs regulated by Sam68 during induction of apoptosis or on the mechanisms involved in this process has been provided. The results presented herein indicate that regulation of apoptosis by Sam68 involves changes in alternative splicing of its cellular target, Bcl-x. We provide evidence that Sam68 binds to endogenous Bcl-x mRNA and that fluctuations in the intracellular levels of this RNA-binding protein affect the ratio between the antiapoptotic Bcl-x(L) and the proapoptotic Bcl-x(s) mRNA. Finally, by using multiple experimental approaches, we show that posttranslational modifications and point mutations affect both the splicing activity of Sam68 toward Bcl-x and induction of apoptosis in live cells. Our work provides the first cellular target of Sam68 involved in apoptosis and suggests a mechanism of action for this RNA-binding protein in response to an altered intracellular environment.

The cellular targets of Sam68 potentially involved in apoptosis were identified by coimmunoprecipitation experiments. Using this approach, we have recently identified additional mRNAs that are targets of Sam68 in mouse male germ cells (Paronetto et al., 2006). The specificity of the binding was assessed by a parallel immunoprecipitation with preimmune IgGs and by confirmation of the targets identified in pull-down assays using purified proteins and RNAs. More important, we show that fluctuations in Sam68 intracellular levels achieved by RNAi or transient transfection profoundly affect alternative splicing of one of these targets: Bcl-x. An increase of Sam68 shifts the balance toward the proapoptotic Bcl-x(s) isoform, and there is a correlation between Sam68-induced Bcl-x(s) splicing and apoptosis. However, as Sam68 binds the mRNAs for other regulators of apoptosis, it is possible that its effects on cell death also involve the regulation of additional targets.

STAR proteins are thought to link signal transduction pathways to mRNA processing (Vernet and Artzt, 1997). Indeed, it was recently shown that ser/thr phosphorylation of Sam68 by Erk1/2 affected exon v5 inclusion in the CD44

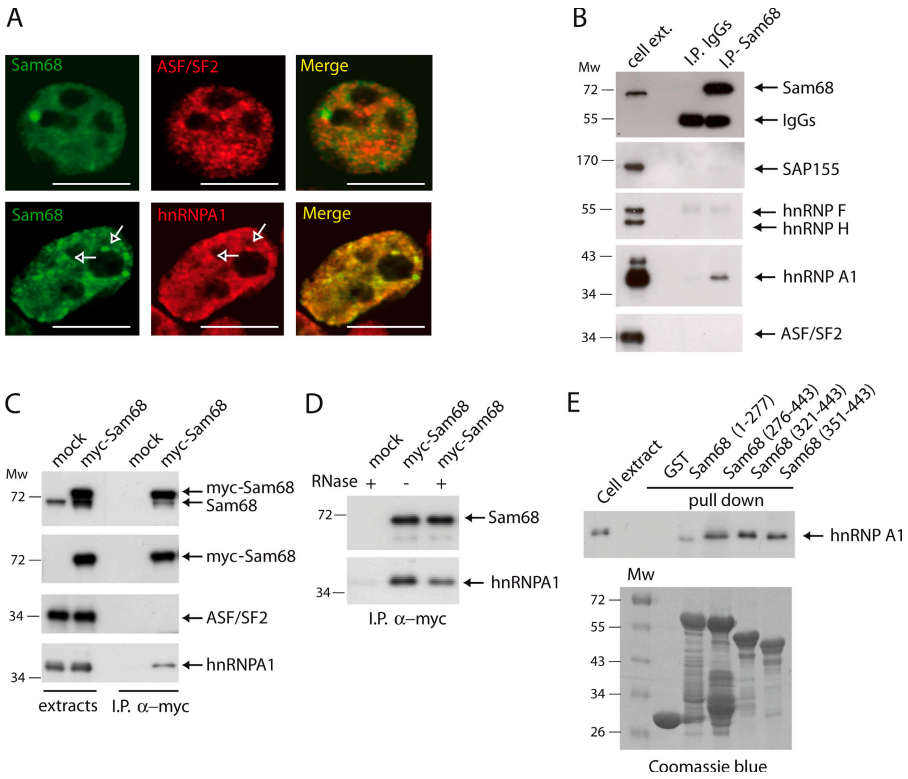

Figure 7. **Sam68 associates with hnRNP A1 in HEK293 cells.** (A) Confocal images of GFP-Sam68 and endogenous ASF/SF2 (top) or hnRNP A1 (bottom). Arrows in the bottom panels show perinucleolar foci in which Sam68 and hnRNP A1 colocalize. Bars, 10 μm. (B) Western blot analysis of the coimmunoprecipitation between endogenous Sam68 or myc-Sam68 (C) and the indicated endogenous splicing factors. (D) Western blot analysis of the association between Sam68 and hnRNP A1 in the presence of RNase. (E) Pull-down assay of hnRNP A1 with GST fusion proteins of fragments of Sam68. (top) Anti–hnRNP A1 Western blot; (bottom) Coomassie blue staining of the same samples.

mRNA (Matter et al., 2002). Surprisingly, we found that Erk1/2 signaling does not strongly affect Sam68-mediated alternative splicing of Bcl-x, suggesting that posttranslational modifications of this RNA-binding protein may differentially regulate its mRNA targets. By contrast, we found that tyrosine phosphorylation of Sam68 by the Src-like kinase Fyn reverts the ratio of Bcl-x(s)/Bcl-x(L) induced by Sam68 and promote the expression of the antiapoptotic Bcl-x(L) mRNA. The same effect was also achieved by creating the V229F substitution or by fusing an RS domain to Sam68. Intriguingly, in all these cases, the localization of Sam68 changed from being diffuse in the nucleoplasm to accumulating in discrete subnuclear foci that are different from the speckles where SC35 and ASF/SF2 accumulate. These observations suggest that Sam68 is in a dynamic equilibrium in the nucleus and that posttranslational modifications affect both the localization and the activity of the protein, resulting in alternative processing of its pre-mRNA targets.

The activity of Src-like kinases is often up-regulated in cancer cells and contributes to cell proliferation, survival, and invasiveness (Irby and Yeatman, 2000). Src activity is up-regulated in human prostate carcinomas at advanced stages, and it correlates with tyrosine phosphorylation of Sam68 (Paronetto et al., 2004). A similar observation was made in breast cancer cells (Lukong et al., 2005), suggesting that it is a common mechanism of control of this protein in neoplastic cells. Our results provide a possible explanation for these observations. Tyrosine phosphorylation of Sam68 in cancer cells may protect them from apoptosis by altering the Bcl-x(s)/Bcl-x(L) ratio in favor of Bcl-x(L) (Fig. 3). In line with this hypothesis, it has been shown that Bcl-x(L) levels are increased in more aggressive prostate cancer cells and that their treatment with synthetic oligonucleotides that promote the Bcl-x(s) splice site selection in the pre-mRNA triggers apoptosis (Mercatante et al., 2002). It is possible that Sam68 participates in the mechanisms that render prostate cancer cells more resistant to apoptosis and that treatments affecting tyrosine phosphorylation of Sam68 can influence survival of cancer cells expressing high levels of Bcl-x(L).

The experiments presented herein demonstrate for the first time that Sam68 can interact with hnRNP A1. Interestingly, we found that tyrosine phosphorylation by Fyn, or mutations like V229F and fusion to a RS domain, disrupted this complex and affected Bcl-x(s) splicing. Moreover, depletion of hnRNP A1 by RNAi strongly attenuated Sam68-induced Bcl-x(s) splicing and apoptosis, suggesting that the interaction between Sam68 and hnRNP A1 is functionally relevant. The interaction between Sam68 and hnRNP A1 is only in part mediated by RNA, suggesting that these proteins could bind cooperatively to pre-mRNAs. Thus, hnRNP A1 might be recruited to certain pre-mRNA regions by the presence of Sam68 in the vicinity. Although future mechanistic experiments are required to define this functional interaction, we hypothesize that Sam68 may affect Bcl-x splicing by attracting hnRNP A1, which is known to compete with ASF/SF2 and to cause switches in 5′ splice sites (Eperon et al., 2000). Generally, there are rather few proteins that influence splice site selection, compared with the number of regulated alternative splice events. It has been postulated that the choice of splice sites is governed by combinations of splice factors, rather than individual proteins (Matlin et al., 2005; Singh and Valcarcel, 2005), but practical examples of interactions between splice factors remain few. Thus, the interaction of Sam68, a tightly regulated RNA-binding protein, with

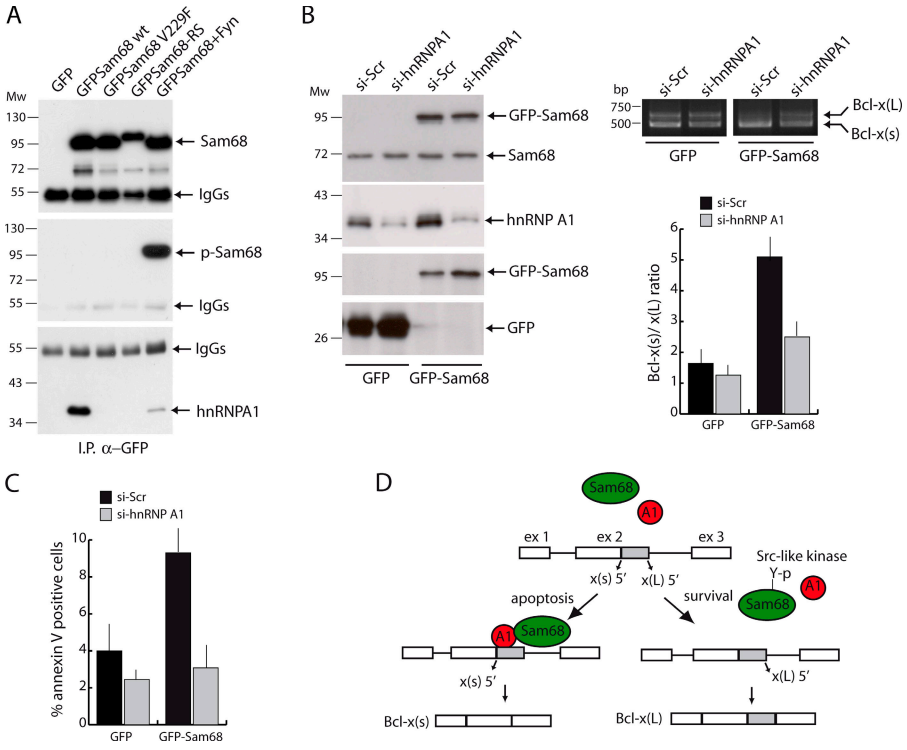

Figure 8. **hnRNP A1 expression favors Sam68-mediated Bcl-x(s) splicing.** (A) Western blot analysis of the coimmunoprecipitation between wild-type or mutant GFP-Sam68 and endogenous hnRNP A1 in the presence or absence of Fyn. (B) Bcl-x minigene splicing assays in HEK293 cells transfected with scrambled (scr) or hnRNP A1 siRNAs and either GFP or GFP-Sam68. (top) Western blot analyses of extracts from the same cells used in the right panel for the splicing assay. The bar graph reports the densitometric analyses of the three experiments performed (mean ± SD). (C) Cells transfected as reported in B, but without the Bcl-x minigene, were stained for annexin V and analyzed by FACS. Data are reported as the mean ± SD of three independent experiments. (D) Hypothetical model of the effects played by Sam68 and hnRNP A1 on Bcl-x alternative splicing.

an abundant factor that has a function in splice site selection, may well become a paradigm in regulated alternative splicing.

In conclusion, the experiments presented herein demonstrate that Sam68 affects the alternative splicing of Bcl-x pre-mRNA and suggest that perturbations of intracellular signaling pathways affecting its tyrosine phosphorylation status can finely tune the splicing activity of Sam68 and predispose the cell to survive or to undergo programmed cell death.

Materials and methods

Plasmid constructs

The Bcl-x minigene has been described previously (Massiello, et al., 2004). The cDNA of human Sam68 was subcloned from pcDNA3-Sam68 (Paronetto, et al., 2003) into EcoRI–SalI restriction site of pEGFP. Site-directed mutations were inserted by PCR using oligonucleotides containing the mutated residue (Fig. S4, available at http://www.jcb.org/cgi/content/full/jcb.200701005/DC1). Wild-type and mutated Sam68 cDNAs were also subcloned into pCDNA3-myc eukaryotic expression vector. The human ASF/SF2 cDNA (available from GenBank/EMBL/DDBJ under accession no. NM_006924) was amplified by RT-PCR using Proofstart polymerase (Pfu; Stratagene) and HEK293 RNA. The cDNA was subcloned into SalI–XbaI restriction sites of p3XFLAG (Sigma-Aldrich). GFP-Sam68-RS was generated by fusing the RS domain of ASF/SF2 (aa 194–248) to the C terminus of Sam68. The cDNA encoding the RS domain of ASF/SF2 was amplified by PCR and subcloned into SalI–BamHI restriction sites of pEGFP in fusion with Sam68 upstream of the TAA codon. All cDNAs used in the experiments were sequenced by Cycle Sequencing (BMR Genomics). Expression vector for Sam68m1, containing the phosphorylation mutated sites, was provided by H. Konig (Institut für Toxikologie und Gnetik, Karlsruhe, Germany).

Cell cultures and transfections

HEK293 cells were maintained in DME (Invitrogen) supplemented with 10% FBS (BioWhittaker Cambrex Bioscience), penicillin, and streptomycin. For transfections, HEK293 cells were plated in 35-mm dishes 1 d before and transfected with 1 μg of DNA (Bcl-x minigene, pEGFP-Sam68$_{wt}$, pEGFP-Sam68$_{V229F}$, pEGFP-Sam68$_{NLSKO}$, pEGFP-Sam68RS, pFLAG-Asf/SF2, pCMV5-Fyn, pCMV5-Fyn$_{Y528F}$, pCDNA3-MEKK1, pCDNA3-myc-Sam68, pCDNA3-myc-Sam68$_{V229F}$) using lipofectamine 2000 (Invitrogen) according to the manufacturer's instructions. At 24 h after transfections, cells were collected for RNA or biochemical analysis. For RNAi, cells at ~50/60% confluence were transfected with siRNAs (MWG Biotech) using Oligofectamine and Opti-MEM medium (Invitrogen). Transfections were performed for 2 or 3 consecutive days. Sequences for Sam68 and hnRNP A1 siRNAs are listed in Fig. S4. Transfection of antisense Bcl-x(L) oligonucleotide (Calbiochem) was performed as for RNAi using Oligofectamine.

Extraction of RNA and proteins from cultured cells

Total RNA was extracted from transfected HEK293 cells using cold Trizol reagent (Invitrogen), according to the manufacturer's instructions. RNA was resuspended in RNase-free water (Sigma-Aldrich) and immediately frozen at −80°C for further analysis.

For protein extraction, HEK293 cells were resuspended in lysis buffer (100 mM NaCl, 10 mM $MgCl_2$, 30 mM Tris-HCl, pH 7.5, 1 mM dithiothreitol, 10 mM β-glycerophosphate, 0.5 mM $NaVO_4$, and protease inhibitor cocktail [Sigma-Aldrich]) supplemented with 0.5% Triton X-100. The extracts were centrifuged for 10 min at 12,000 *g* at 4°C, and the supernatants were collected and used for Western blot or immunoprecipitation experiments.

Immunoprecipitation experiments

HEK293 cells were homogenized in lysis buffer (100 mM NaCl, 10 mM $MgCl_2$, 30 mM Tris-HCl, 1 mM DTT, protease inhibitor cocktail, and 40 U/ml RNase OUT [Invitrogen]) supplemented with 0.5% Triton X-100. Soluble extracts were separated by centrifugation at 10,000 *g* for 10 min, and they were precleared for 2 h on protein A–Sepharose beads (Sigma-Aldrich) in the presence of 2 μg rabbit IgGs, 0.05%BSA, and 0.1 μg/ml yeast tRNA. After centrifugation for 1 min at 1,000 *g*, supernatants were incubated with 2 μg anti-Sam68 (Santa Cruz Biotechnology, Inc.), anti-GFP (Roche), or rabbit IgGs for 3 h at 4°C under constant rotation. Beads were washed three times with lysis buffer, and an aliquot was eluted in SDS sample buffer for Western blot analysis. The remaining beads were incubated with lysis buffer in the presence of (RNase-free) DNase (Roche) for 15 min at 37°C and washed three times with lysis buffer before incubation with 50 μg proteinase K (Roche) for an additional 15 min at 37°C. Co-precipitated RNA was then extracted by standard procedure and used for RT-PCR using BclX-1 and rtBclX-2 primers (Fig. S4). For the coimmunoprecipitation experiment with hnRNP A1, nuclear extracts were prepared by resuspending cells in ipotonic buffer (10 mM Tris/HCl, pH 7.4, 10 mM NaCl, 2.5 mM $MgCl_2$, 1 mM DTT, protease inhibitor cocktail, 30 U/ml RNase OUT,

10 mM β-glycerophosphate, and 0.5 mM $NaVO_4$). After incubation on ice for 7 min, samples were centrifuged at 700 *g* for 7 min. Pelleted nuclei were resuspended in ipotonic buffer supplemented with 90 mM NaCl and 0.5% Triton X-100, sonicated, and stratified on 30% sucrose. After a centrifugation at 5,000 *g* for 15 min, nuclear extracts were precleared and immunoprecipitated as described. Where indicated, nuclear extracts were treated with 100 μg/ml RNase A (Sigma-Aldrich).

GST pull-down assay of the mRNA–Sam68 and protein–protein interactions

For protein–protein interactions, GST and GST-Sam68 were purified from *Escherichia coli* as previously described (Sette et al., 1998) and incubated for 1 h with nuclear extracts. For RNA–protein interactions, 2 μg of purified GST proteins were equilibrated for 1 h in 50 mM Tris-HCl, pH 7.4, 100 mM KCl, 2 mM $MgCl_2$, 1 mM EDTA, 1 mM DTT, 40 U/ml RNase OUT, and 0.2% Nonidet-P40 supplemented with 0.05% BSA and 0.1 μg/ml yeast tRNA. Purified total RNA from HEK293 was added to the beads and incubated at 4°C under constant rotation. Beads were washed and RNA was extracted as described in the previous paragraph.

RT-PCR analysis

1 μg of RNA from HEK293 transfected cells or all of the coimmunoprecipitated RNA was used for RT-PCR using M-MLV reverse transcriptase (Invitrogen) according to manufacturer's instructions. 10% of the reverse-transcription reaction was used as template together with the following primers: endogenous Bcl-x, Bcl-X-1 (forward) and Bcl-X-2 (reverse); real-time PCR, rt-BclX-1 (forward) and rt-BclX-2 (reverse); Bcl-x minigene, mg-BclX-1 (forward) and mg-BclX-2 (reverse). All primer sequences are listed in Fig. S4. Real-time PCR was performed using the iQ Sybr-green Supermix (Bio-Rad Laboratories) according to manufacturer's instructions.

Western blot analysis

Cell extracts or immunoprecipitated proteins were diluted in SDS sample buffer and boiled for 5 min. Proteins were separated on 10% SDS-PAGE gels and transferred to Hybond-P membranes (GE Healthcare) as previously described (Sette et al., 2002). The following primary antibodies (1:1,000 dilution) were used (overnight at 4°C): rabbit anti-Sam68, rabbit anti-Erk2, rabbit anti-Fyn, and mouse anti-phosphotyrosine (PY20; Santa Cruz Biotechnology, Inc.); mouse anti-ASF/SF2 (US Biological); mouse anti–hnRNP A1, mouse anti-tubulin, and rabbit anti-actin (Sigma-Aldrich); mouse anti–hnRNP H/F (Abcam); rabbit anti–phospho-ERKs (Cell Signaling); rabbit anti-GFP (Roche); rabbit anti-phosphoserine and anti-phosphothreonine (Stressgen); and rabbit anti–Bcl-x (BD Biosciences). Secondary anti-mouse or anti-rabbit IgGs conjugated to horseradish peroxidase (GE Healthcare) were incubated with the membranes for 1 h at room temperature at a 1:10,000 dilution in PBS containing 0.1% Tween 20. Immunostained bands were detected by chemiluminescent method (Santa Cruz Biotechnology, Inc.).

Annexin V staining

Transfected cells grown on 35-mm plates were harvested and processed for annexin V staining or for Western blot analysis. For annexin V staining, cells were washed in PBS and stained with the annexin V–PE (BD Biosciences) according to the manufacturer's instructions. GFP-positive cells were then analyzed with a FACSCalibur Flow Cytometer (Becton Dickinson).

Immunofluorescence analysis

Transfected HEK293 cells were fixed in 4% paraformaldehyde and washed three times with PBS. Cells were permeabilized with 0.1% Triton X-100 for 7 min and incubated for 1 h in 0.5% BSA. Cells were washed three times with PBS and incubated for 2 h at room temperature with antibodies against cleaved casp3 (1:400; Sigma-Aldrich), SC35 (1:200; Sigma-Aldrich), Asf /SF2 (1:100), or hnRNP A1 (1:400), followed by 1 h of incubation with cy3-conjugated anti-mouse IgGs (Chemicon). After washes, slides were mounted with MOWIOL reagent (Calbiochem) and analyzed by confocal microscopy using an inverted microscope (Carl Zeiss MicroImaging, Inc.).

Image acquisition and manipulation

Images in Fig. 3 A, Fig. 4 A, Fig. 6 A, and Fig. S1 A were taken from an inverted microscope (IX70; Olympus) using an LCA ch 20×/0.40 objective. Images in Fig. 5 B were taken from a microscope (Axioskop; Carl Zeiss MicroImaging, Inc.) using a Pan-Neofluar 40×/0.75 objective. Images were acquired at room temperature using a RT-slider camera (Diagnostic Instruments) and the IAS2000 software (Biosistem82; Delta Sistemi). The confocal images in Fig. 7 A and Fig. S3 were taken from a confocal microscope (LSM510; Carl Zeiss MicroImaging, Inc.) using a Plan-Neofluar 40×/1.3 oil differential interference contrast objective and the LSM510 software (Carl Zeiss MicroImaging, Inc.). Images were acquired as TIFF files, and Photoshop and Illustrator (Adobe) were used for composing the panels.

Online supplemental material

Fig. S1 shows that the ERK1/2 pathway does not regulate Sam68-mediated alternative splicing of Bcl-x. Fig. S2 shows the effects of overexpressed Fyn on the alternative splicing of endogenous Bcl-x transcripts. Fig. S3 shows the localization of Sam68 mutants and splicing regulators in HEK293 cells. Fig. S4 shows a list of the oligonucleotides used for the PCR reactions in the article. Online supplemental material is available at http://www.jcb.org/cgi/content/full/jcb.200701005/DC1.

The authors wish to thank Professor Raffaele Geremia for his support and advice during this work. We are also indebted to Dr. Harald Konig for the gift of the myc-Sam68m1 construct and Dr. Ezio Giorda, Rita Carsetti, Daniela Angelini, and Luca Battistini for their help and suggestions with FACS analysis.

M.P. Paronetto was supported by a postdoctoral fellowship from the Istituto di Ricovero e Cura a Carattere Scientifico Fondazione Santa Lucia. This work was supported by grants from Telethon (GGP418), the Associazione Italiana Ricerca sul Cancro, and the Italian Ministry of Education (PRIN 2004 and PRIN2006) to C. Sette and by a National Institutes of Health grant (RO1 HL072925) to C.E. Chalfant.

Submitted: 2 January 2007
Accepted: 13 February 2007

References

Babic, I., E. Cherry, and D.J. Fujita. 2006. SUMO modification of Sam68 enhances its ability to repress cyclin D1 expression and inhibits its ability to induce apoptosis. *Oncogene.* 25:4955–4964.

Batsché, E., M. Yaniv, and C. Muchardt. 2006. The human SWI/SNF subunit Brm is a regulator of alternative splicing. *Nat. Struct. Mol. Biol.* 13:22–29.

Black, D.L. 2003. Mechanisms of alternative pre-messenger RNA splicing. *Annu. Rev. Biochem.* 72:291–336.

Boise, L.H., M. Gonzalez-Garcia, C.E. Postema, L. Ding, T. Lindsten, L.A. Turka, X. Mao, G. Nunez, and C.B. Thompson. 1993. *bcl-x*, a *bcl-2*-related gene that functions as a dominant regulator of apoptotic cell death. *Cell.* 74:597–608.

Chalfant, C.E., K. Rathman, R.L. Pinkerman, R.E. Wood, L.M. Obeid, B. Ogretmen, and Y.A. Hannun. 2002. De novo ceramide regulates the alternative splicing of caspase 9 and Bcl-x in A549 lung adenocarcinoma cells. Dependence on protein phosphatase-1. *J. Biol. Chem.* 277:12587–12595.

Chen, T., F.M. Boisvert, D.P. Bazett-Jones, and S. Richard. 1999. A role for the GSG domain in localizing Sam68 to novel nuclear structures in cancer cell lines. *Mol. Biol. Cell.* 10:3015–3033.

Cheng, C., and P.A. Sharp. 2006. Regulation of CD44 alternative splicing by SRm160 and its potential role in tumor cell invasion. *Mol. Cell. Biol.* 26:362–370.

Clarke, M.F., I.J. Apel, M.A. Benedict, P.G. Eipers, V. Sumantran, M. Gonzalez-Garcia, M. Doedens, N. Fukunaga, B. Davidson, J.E. Dick, et al. 1995. A recombinant bcl-x s adenovirus selectively induces apoptosis in cancer cells but not in normal bone marrow cells. *Proc. Natl. Acad. Sci. USA.* 92:11024–11028.

Cote, J., F.M. Boisvert, M.C. Boulanger, M.T. Bedford, and S. Richard. 2003. Sam68 RNA binding protein is an in vivo substrate for protein arginine N-methyltransferase 1. *Mol. Biol. Cell.* 14:274–287.

Eperon, I.C., O.V. Makarova, A. Mayeda, S.H. Munroe, J.F. Caceres, D.G. Hayward, and A.R. Krainer. 2000. Selection of alternative 5′ splice sites: role of U1 snRNP and models for the antagonistic effects of SF2/ASF and hnRNP A1. *Mol. Cell. Biol.* 20:8303–8318.

Fumagalli, S., N.F. Totty, J.J. Hsuan, and S.A. Courtneidge. 1994. A target for Src in mitosis. *Nature.* 368:871–874.

Garneau, D., T. Revil, J.F. Fisette, and B. Chabot. 2005. Heterogeneous nuclear ribonucleoprotein F/H proteins modulate the alternative splicing of the apoptotic mediator Bcl-x. *J. Biol. Chem.* 280:22641–22650.

Irby, R.B., and T.J. Yeatman. 2000. Role of SRC expression and activation in human cancer. *Oncogene*. 19:5636–5642.

Jones, A.R., and T. Schedl. 1995. Mutations in gld-1, a female germ cell-specific tumor suppressor gene in *Caenorhabditis elegans*, affect a conserved domain also found in Src-associated protein Sam68. *Genes Dev.* 9:1491–1504.

Li, X., J. Wang, and J.L. Manley. 2005. Loss of splicing factor ASF/SF2 induces G2 cell cycle arrest and apoptosis, but inhibits internucleosomal DNA fragmentation. *Genes Dev.* 19:2705–2714.

Lin, Q., S.J. Taylor, and D. Shalloway. 1997. Specificity and determinants of Sam68 RNA binding. Implications for the biological function of K homology domains. *J. Biol. Chem.* 272:27274–27280.

Lukong, K.E., and S. Richard. 2003. Sam68, the KH domain-containing superSTAR. *Biochim. Biophys. Acta.* 1653:73–86.

Lukong, K.E., D. Larocque, A.L. Tyner, and S. Richard. 2005. Tyrosine phosphorylation of sam68 by breast tumor kinase regulates intranuclear localization and cell cycle progression. *J. Biol. Chem.* 280:38639–38647.

Maniatis, T., and B. Tasic. 2002. Alternative pre-mRNA splicing and proteome expansion in metazoan. *Nature.* 418:236–243.

Mercatante, D.R., J.L. Mohler, and R. Kole. 2002. Cellular response to an antisense-mediated shift of Bcl-x pre-mRNA splicing and antineoplastic agents. *J. Biol. Chem.* 277:49374–49382.

Massiello, A., A. Salas, R.L. Pinkerman, P. Roddy, J.R. Roesser, and C.E. Chalfant. 2004. Identification of two RNA cis-elements that function to regulate the 5′ splice site selection of Bcl-x pre-mRNA in response to ceramide. *J. Biol. Chem.* 279:15799–15804.

Massiello, A., J.R. Roesser, and C.E. Chalfant. 2006. SAP155 binds to ceramide-responsive RNA cis-element 1 and regulates the alternative 5′ splice site selection of Bcl-x pre-mRNA. *FASEB J.* 20:1680–1682.

Matlin, A.J., F. Clark, and C.W. Smith. 2005. Understanding alternative splicing: towards a cellular code. *Nat. Rev. Mol. Cell Biol.* 6:386–398.

Matter, N., P. Herrlich, and H. Konig. 2002. Signal-dependent regulation of splicing via phosphorylation of Sam68. *Nature.* 420:691–695.

Olopade, O.I., M.O. Adeyanju, A.R. Safa, F. Hagos, R. Mick, C.B. Thompson, and W.M. Recant. 1997. Overexpression of BCL-x protein in primary breast cancer is associated with high tumor grade and nodal metastases. *Cancer J. Sci. Am.* 3:230–237.

Paronetto, M.P., J. Venables, D. Elliott, R. Geremia, P. Rossi, and C. Sette. 2003. Tr-kit promotes the formation of a multimolecular complex composed by Fyn, PLCγ1 and Sam68. *Oncogene.* 22:8707–8715.

Paronetto, M.P., D. Farini, I. Sammarco, G. Maturo, G. Vespasiani, R. Geremia, P. Rossi, and C. Sette. 2004. Expression of a truncated form of the c-Kit tyrosine kinase receptor and activation of Src kinase in human prostatic cancer. *Am. J. Pathol.* 164:1243–1251.

Paronetto, M.P., F. Zalfa, F. Botti, R. Geremia, C. Bagni, and C. Sette. 2006. The nuclear RNA-binding protein Sam68 translocates to the cytoplasm and associates with the polysomes in mouse spermatocytes. *Mol. Biol. Cell.* 17:14–24.

Pelisch, F., M. Blaustein, A.R. Kornblihtt, and A. Srebrow. 2005. Cross-talk between signaling pathways regulates alternative splicing: a novel role for JNK. *J. Biol. Chem.* 280:25461–25469.

Schumacher, B., M. Hanazawa, M.H. Lee, S. Nayak, K. Volkmann, E.R. Hofmann, M. Hengartner, T. Schedl, and A. Gartner. 2005. Translational repression of *C. elegans* p53 by GLD-1 regulates DNA damage-induced apoptosis. *Cell.* 120:357–368.

Schwerk, C., and K. Schultze-Osthoff. 2005. Regulation of apoptosis by alternative pre-mRNA splicing. *Mol. Cell.* 19:1–13.

Sette, C., A. Bevilacqua, R. Geremia, and P. Rossi. 1998. Involvement of phospholipase Cγ1 in mouse egg activation induced by a truncated form of the C-kit tyrosine kinase present in spermatozoa. *J. Cell Biol.* 142:1063–1074.

Sette, C., M.P. Paronetto, M. Barchi, A. Bevilacqua, R. Geremia, and P. Rossi. 2002. Tr-kit-induced resumption of the cell cycle in mouse eggs requires activation of a Src-like kinase. *EMBO J.* 21:5386–5395.

Singh, R., and J. Valcarcel. 2005. Building specificity with nonspecific RNA-binding proteins. *Nat. Struct. Mol. Biol.* 12:645–653.

Stetefeld, J., and M.A. Ruegg. 2005. Structural and functional diversity generated by alternative mRNA splicing. *Trends Biochem. Sci.* 30:515–521.

Taylor, S.J., and D. Shalloway. 1994. An RNA-binding protein associated with Src through its SH2 and SH3 domains in mitosis. *Nature.* 368:867–871.

Taylor, S.J., R.J. Resnick, and D. Shalloway. 2004. Sam68 exerts separable effects on cell cycle progression and apoptosis. *BMC Cell Biol.* 5:5–16.

Vernet, C., and K. Artzt. 1997. STAR, a gene family involved in signal transduction and activation of RNA. *Trends Genet.* 13:479–484.

Wang, L.L., S. Richard, and A.S. Shaw. 1995. P62 association with RNA is regulated by tyrosine phosphorylation. *J. Biol. Chem.* 270:2010–2013.

Wu, J., L. Zhou, K. Tonissen, R. Tee, and K. Artzt. 1999. The quaking I-5 protein (QKI-5) has a novel nuclear localization signal and shuttles between the nucleus and the cytoplasm. *J. Biol. Chem.* 274:29202–29210.